Colloid Polym Sci (2015) 293:35–48
DOI 10.1007/s00396-014-3388-4

ORIGINAL CONTRIBUTION

Supramolecular organogels based on perylenetetracarboxylic diimide trimers linked with benzenetricarboxylate

Chengguang Gao · Lin Xue · Yuhan Chen · Xiyou Li

Received: 23 July 2014 / Revised: 17 August 2014 / Accepted: 28 August 2014 / Published online: 11 September 2014

Abstract Two new perylenetetracarboxylic diimide (PDI) derivatives, namely, trimer **1** and trimer **2**, composed of three PDI units with different tail groups, are prepared. Solubility of these two trimers is significantly different due to the different tail groups. The aggregation behavior of these two compounds in solution was investigated using absorption and fluorescence spectra. The results indicate that both trimers **1** and **2** can form large molecular aggregates via an intermolecular process in either good solvent or poor solvent. Trimer **1** can form gel in a mixed solvent of methanol and tetrahydrofuran (THF), while trimer **2** can only form gel in non-polar solvents, such as hexane and toluene. This can be ascribed to the multiple long alkyl chains in trimer **2**, which have introduced extra hydrophobic interactions besides the π–π interactions between the molecules of trimer **2**. The morphology examination of the dried gel of trimer **1** by atomic force microscopy (AFM) reveals simply long fibers. But, the dried gel of timer **2** shows network-like morphology, which can be ascribed to the hydrophobic interactions between the multiple alkyl chains.

Keywords Organic gel · Perylene diimide · Absorption spectrum · Fluorescence spectrum

Electronic supplementary material The online version of this article (doi:10.1007/s00396-014-3388-4) contains supplementary material, which is available to authorized users.

C. Gao · Y. Chen · X. Li (✉)
Key Laboratory of Colloid and Interface Chemistry of Ministry of Education, Department of Chemistry, Shandong University, Jinan, China 250100
e-mail: xiyouli@sdu.edu.cn

L. Xue
Environmental Protection Bureau of Laiwu City, Laiwu, China 271100

Introduction

Supramolecular organic assembly have attracted a lot of research interests due to their numerous potential application in many fields, such as semiconductors in electronic devices [1–4], functional materials in photovoltaic [5–8] devices, liquid crystals [9, 10], and artificial biological materials (artificial muscles [11], synthetic membranes[12], and cell growth [13]). They also offer the possibility in some cases to organize hierarchical nanostructures [14, 15]. Moreover, organic gels, an important group of molecular self-assembly, can also provide unique environment for photochemical or photophysical process because of the special gel state [16, 17].

As an important group of molecular self-assembly, organic gels have attracted a lot of research attentions recently [18]. The formation of organogel is ascribed to the formation of molecular self-assembly in solution driven by non-covalent interactions, such as π–π stacking, hydrogen bonding, metal-ion coordination, dipole–dipole interactions, and other van der Waals interactions. Recently, organogelators based on porphyrins [19–23], phthalocyanines [24, 25], and conjugate oligomers [26, 27] in pure or mixed solutions have been developed. Perylenetetracarboxylic diimide (PDI) derivatives became a kind of popular building block for organic gels recently, because of their excellent thermal and light stabilities and great application potentials as photonic materials [28]. Sinkai reported a mixed gel of PDI derivatives with different substituents at the bay positions and found sequenced energy transfer in this gel [17]. Rybtchinski and co-workers prepared a supramolecular gel based on an amphiphilic PDI, which can response to the outside stimuli [29]. Würthner and co-workers have reported a highly fluorescent organic gel based on a PDI derivative functionalized with urea groups [30]. It is found that the π–π interactions dominate the formation process of gel. The aggregation model (H- or J-type) plays a crucial role in determining the properties of the gels [31, 32]. We have

found that introduction of multiple aromatic subunits in one gelator molecule could increase the interactions among the molecules significantly, which is believed to be favorable for a gelator [33]. A porphyrin trimer linked with a 1,3,5-benzenetricarboxylate bridge can form a well-defined pattern on a mica or glass surface via self-assembling [34]. This result suggested that linking chromophores with 1,3,5-benzenetricarboxylate to form trimers might be a good strategy to enforce the interactions among the molecules and achieve a good gelator.

In this work, we prepared two new PDI trimers linked with 1,3,5-tricarboxylate benzene, namely, trimers **1** and **2**, as shown in Fig. 1. Different tail groups are linked for the purpose of changing their solubility in different organic solvents. The aggregation behaviors of these two compounds in solution are investigated by the steady-state absorption and fluorescence spectra. The gelating properties of them in different solvents are also tested. The structures of the dried gels are determined by the X-ray diffraction (XRD) experiments, and the morphology is examined by atomic force microscopy.

Results and discussion

Molecular design and synthesis

PDIs with no substituent at the bay positions have very strong π–π interactions and, therefore, are ideal building blocks for the construction of ordered molecular aggregates [35]. However, the low solubility of these no-substituted PDIs in conventional organic solvents brings difficulties to the synthesis and purifications. Therefore, we choose 1,7-diphenoxyl substituted PDIs as the building block of our compounds, which can maintain a reasonable solubility in conventional organic solvents and a strong π–π interaction between each other simultaneously [36, 37]. The tris(dodecyloxy)benzamide group in trimer **2** could improve the solubility of it in conventional organic solvents, especially in non-polar organic solvents. Meanwhile, it can also bring hydrophobic interaction among the long alkyl chains of the different molecules, which are expected to promote the molecular order in the aggregates efficiently.

The synthetic procedures of these two trimers are shown in Scheme 1. 1,7-Di(p-t-butyl-phenoxyl)-3,4,9,10-tetracarboxylic dianhydride (**5**) [38] reacts first with *n*-hexyl amine or *N*-(2-aminoethyl)-3,4,5-tris(dodecyloxy)benzamide [34] in refluxing pyridine to give the key intermediate monoanhydried PDI **6** or **7**. Further reaction of **6** or **7** with ethylenediamine gives intermediate **8** or **9**. In the last step, the benzoylation of **8** or **9** with trimesoyl chloride gives trimers **1** and **2**, respectively, with reasonable yields. These compounds are purified by repeat column chromatography on silica with a mixture of chloroform and methanol as eluent; all the new compounds were fully characterized with ^{1}H NMR, matrix-assisted laser desorption/ionization–time-of-flight (MALDI-TOF) mass spectra, and elemental analysis.

UV–vis absorption and fluorescence spectra in solutions

UV–vis absorption and fluorescence spectra of PDIs are sensitive to the interchromophore distance and orientation [39, 40] and, therefore, have been widely used to monitor the π–π

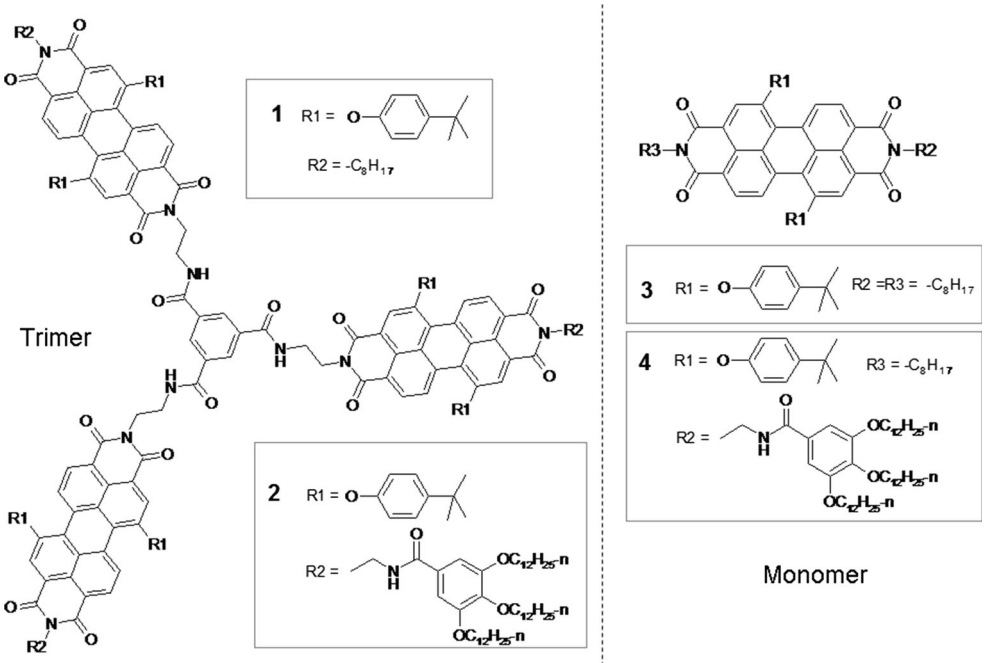

Fig. 1 The molecular structure of trimer **1** and **2**, and monomer **3** and **4**

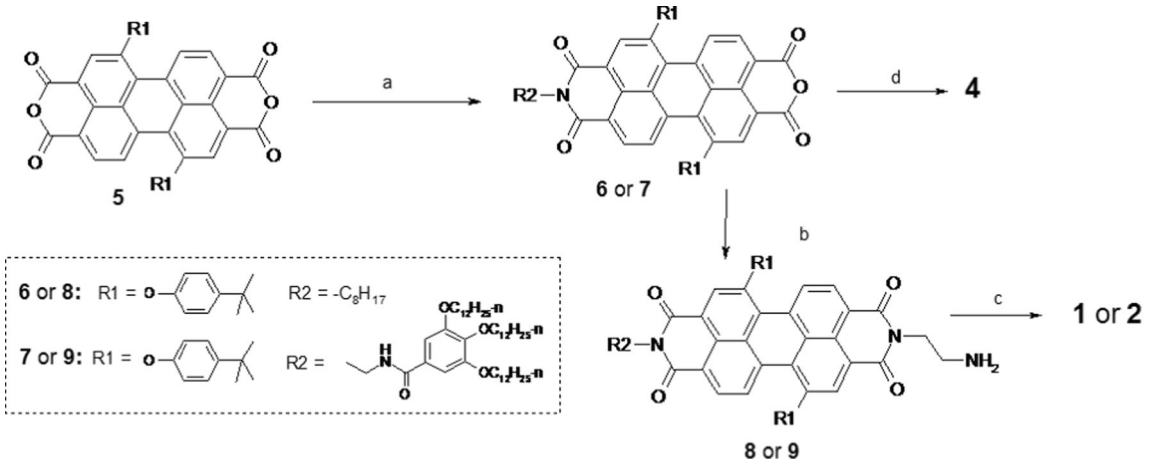

Scheme 1 Synthesis of trimers **1** and **2**. *a* pyridine/reflux; *b* $CHCl_3$, room temperature, ethylenediamine; *c* trimesoyl chloride, $CHCl_3$, room temperature; *d* pyridine/reflux, 1-octylamine

stacking of PDIs [41–43]. Figure 2 compares the absorption and emission spectra of these two trimers in diluted $CHCl_3$ solution with those of monomeric PDI. Because both of these two PDI trimers are very soluble in chloroform, typical monomeric absorption and fluorescence spectra of them in chloroform are expected. The absorption spectra of trimer **1** in a much diluted solution of $CHCl_3$ (5×10^{-7} mol L^{-1}) have indeed resembled those of a monomeric PDI in shape

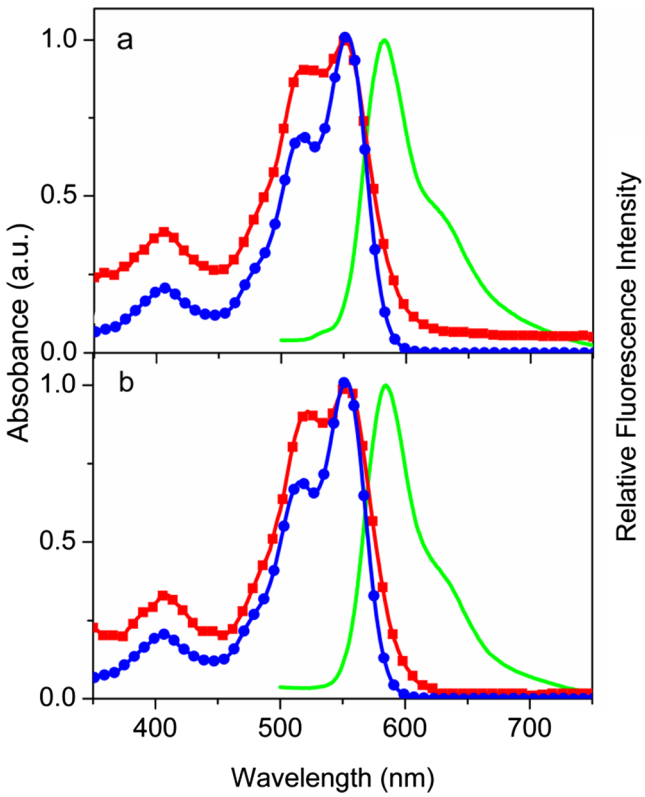

Fig. 2 Normalized absorption (*red*, *solid square*) and emission (*green*, *no symbols*) spectra of trimer **1** (**a**) and trimer **2** (**b**) in diluted $CHCl_3$ (5×10^{-7} mol L^{-1}). The absorption spectrum of monomer **3** (**a**) and **4** (**b**) in diluted $CHCl_3$ (*blue*, *solid circle*) is shown for comparison purpose

(Fig. 2a) [44], with the maximal absorption peak appears at 549 nm and a small shoulder at about 519 nm. The former can be attributed to the 0–0 transition, whereas the later can be assigned to the 0–1 transition. However, the intensity ratio of 0–1 and 0–0 peaks (I_{0-1}/I_{0-0}) is large than that of the monomer **3** PDI (0.69 of monomeric PDI vs 0.90 of trimer **1**). This indicates the presence of "H-type" aggregates of trimer **1** in this diluted solution [45]. An emission band at about 582 nm is found in the fluorescence spectrum of trimer **1**, which is the mirror image of the absorption band. The fluorescence quantum yield of this emission band is about 8.43 %, which is remarkably smaller than that of monomer **3** (98 %) [44]. This is also an evidence for the presence of aggregation of PDI units of trimer **1** in diluted chloroform solution.

The absorption spectrum of trimer **2** in $CHCl_3$ (5×10^{-7} mol L^{-1}) resembled that of monomer **4** (Fig. 2b). The intensity ratio of the 0–1 and 0–2 vibration bands is 0.92, which is almost same as that of trimer **1** and larger than that of monomer **4**, indicating the presence of similar aggregation for trimer **2**. The emission band of trimer **2** appears at 584 nm with a fluorescence quantum yields of 3.89 %. Because several works have reported that there is a photo-induced electron transfer from trialkoxylbenzene group to PDI and then the fluorescence of PDI can be quenched [46]. The low fluorescence quantum yield of timer **2** might be the result of electron transfer. To verify this point, we have also prepared a model compound monomer **4**, which has a trialkoxylbenzene group connected at the imide nitrogen atom. The fluorescence quantum yield of this compound is 86 %, which is smaller than that of monomer **3** (98 %), but still remarkably larger than that of trimer **2**. So the low fluorescence quantum yield of trimer **2** is not caused by electron transfer; it is caused by the aggregation of PDI units. Besides, in the ^1H NMR spectra of trimer **2** (4.5×10^{-4} mol L^{-1}) and **1** ($c=3.0\times10^{-4}$ mol L^{-1}) in $CDCl_3$, very broad peaks were observed, which suggests also the formation of molecular aggregates in the solution.

Now, a critical question is that is the aggregation of timer **1** and **2** in diluted solution an intermolecular process or an intramolecular process? As mentioned above, the absorption spectra are recorded in a solution of chloroform with a concentration of as low as 5×10^{-7} mol L^{-1}. Normally, no intermolecular interaction can be observed in such a dilute solution. Therefore, the aggregates of the PDIs in the trimers as revealed by the absorption spectra are speculated to be caused by an intramolecular aggregation. To verify this point, we recorded the absorption spectra of trimers **1** and **2** in chloroform (5×10^{-7} mol L^{-1}) at different temperatures. Figure 3 shows the temperature-dependent absorption spectra of trimer **1**. It can be found that the absorption spectra of trimer **1** in diluted chloroform have not shown obvious changes along with temperature increase; only a very small shift on the maximal absorption band can be identified, and this may be ascribed to the different solvation effects of chloroform on the solute. The intensity ratio of 0–0 and 0–1 transition has also kept unchanged. This result suggests that the aggregation of the PDI subunits of trimer **1** in diluted solution is not affected by temperature significantly. This is further supported by the temperature-dependent fluorescence spectra of trimer **1**, which revealed no significant changes on emission wavelength and very small increase on the fluorescence quantum yield (Fig. 3b). All these temperature-dependent experiments (including the absorption and fluorescence spectra) revealed that the aggregation of trimer **1** in diluted chloroform solution (5×10^{-7} mol L^{-1}) is an intramolecular aggregation instead of an intermolecular aggregation. The same results can be deduced from the temperature-dependent absorption and

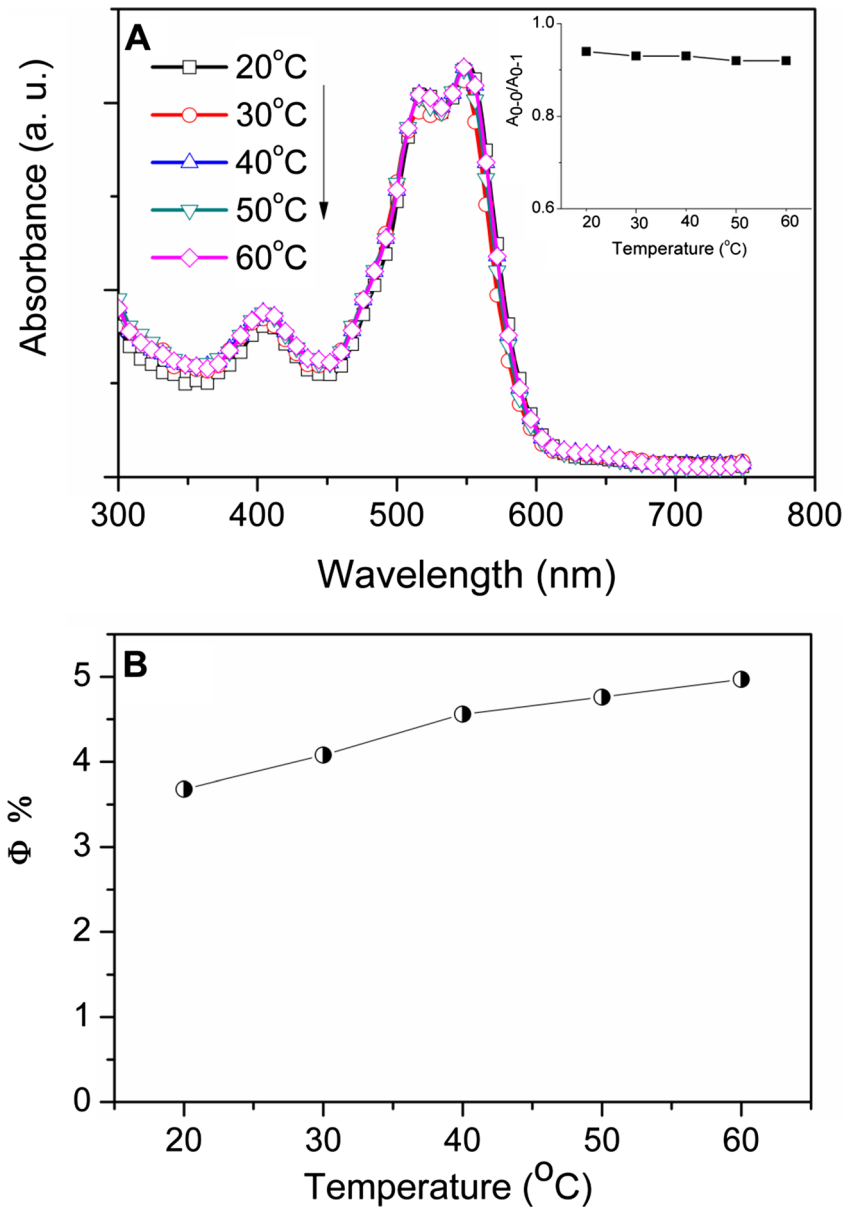

Fig. 3 **a** The absorption spectra of trimer **1** in chloroform (5×10^{-7} mol L^{-1}) at different temperatures (the spectra were recorded in a cell with 5-cm light path). The *inset* shows the peak intensity ratio of A_{0-1}/A_{0-0} at different temperatures. **b** The fluorescence quantum yields of trimer **1** in chloroform (5×10^{-7} mol L^{-1}) at different temperatures

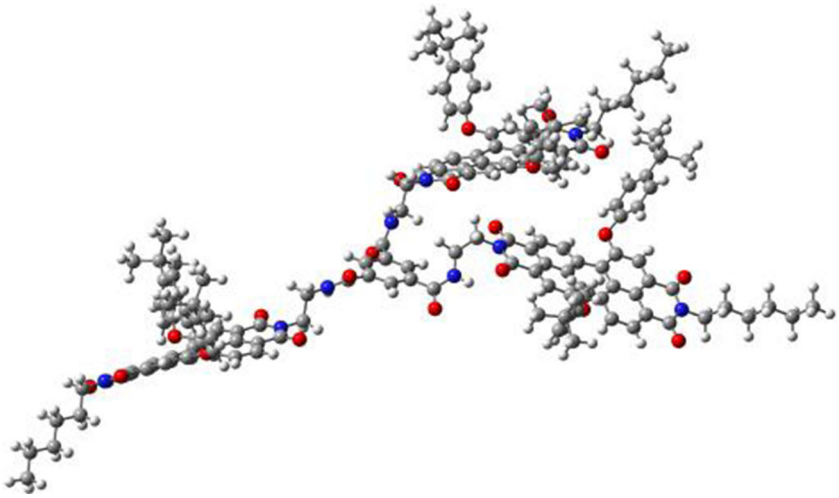

Fig. 4 The minimized molecular structure of trimer **1** with AM1 method. The *right part* shows a pair of PDI subunits stack in a twisted "face-to-face" mode

fluorescence spectra of trimer **2** (Fig. S1 in Supporting Information). We suggest that the intramolecular aggregation of PDI subunits in trimer **1** or **2** is the result of an interbranch interactions as shown in Fig. 4. Because of the flexibility of the linkage between the central phenyl bridge and the PDI subunits, the PDI subunits can take a twisted "face-to-face" stacked structure and show some characteristics of aggregates [47].

When increasing the concentration of trimer **1** in chloroform from 5×10^{-7} to 5×10^{-5} mol L^{-1}, the absorption spectra show significant change along with concentration increase (Fig. 5). The relative intensity ratio of the 0–1 and 0–0 transition increased from 0.90 to 1.1, indicating the formation of the H-type aggregates in concentrated solutions. Because this aggregation is concentration-dependent, therefore, it can be attributed to the intramolecular aggregation. Similar changes on the absorption spectra of trimer **2** are observed along with the concentration increase. However, the relative intensity ratio between the 0–1 and 0–0 bands of trimer **2** increases up to 1.4 when concentration is 5×10^{-5} mol L^{-1}, which is obviously larger than that of trimer **1**. This may be ascribed to the long alkyl chains, which enforce the interactions between the molecules of timer **2**, and the aggregates of trimer **2** are more stable than those of trimer **1** [37]. The intermolecular aggregation of trimers **1** and **2** is also proved by the temperature-dependent absorption spectra (Fig. S2 in Supporting Information). The relative intensity ratio of 0–1 and 0–0 transitions decreases on heating and increases on cooling, which revealed the reversible nature of the intermolecular aggregation process.

The concentration-dependent fluorescence spectra of trimer **1** in chloroform (concentration range 5×10^{-7} to 5×10^{-5} mol L^{-1}) revealed also the presence of intermolecular aggregation (Fig. 6). Along with concentration increase, the emission at 560 nm, the fluorescence of monomeric PDI, disappears gradually. Meanwhile, a broad emission band appears in longer wavelength region. The broad emission at longer wavelength can be attributed to the emission of excimer [48]. The fluorescence quantum yields of trimer **1** decrease obviously along with concentration increase, indicating the formation of intermolecular aggregates. These aggregates can be broken by heating, revealing the reversible nature of the intermolecular aggregation [49]. The concentration and temperature-dependent absorption and fluorescence spectra of trimer **2** (Fig. S3 and S4 in Supporting Information) show similar results with those of trimer **1**, indicating the formation of similar aggregates of trimer **2** in concentrated solutions.

Aggregation in poor solvents

Because the aggregation behavior of PDI is efficiently affected by its solubility in solvents, it is necessary to test the aggregation behavior of the trimers in a solvent with low solubility, i.e., bad solvent. Based on the solubility of trimer **1** and trimer **2** in different solvents, we choose a mixture of methanol and tetrahydrofuran (THF) (V_{MeOH}/V_{THF}=1:4) as solvent for trimer **1** and methyl cyclohexane (MCH) or toluene for trimer **2**.

In the mixed solvent, the absorption spectrum of trimer **1** does not show two vibration bands as that in chloroform, but a broad absorption band with a peak at 512 nm instead (Fig. 7). It can be attributed to the formation of H-type aggregates in this mixed solvent [50]. It is worth noting that the absorption spectrum does not show any changes even though the concentration is reduced to as small as 5×10^{-7} mol L^{-1}; this means that trimer **1** formed very stable aggregates in the mixed solvent (Fig. S4 in Supporting Information). However, the concentration-dependent fluorescence spectra of trimer **1** in this mixed solvent show distinctive changes (Fig. 8). In a diluted solution, two emission bands with peaks at 560 and 650 nm, respectively, can be identified from the fluorescence spectra. But, the emission peak at 560 nm disappeared gradually along with concentration increase. The emission at 560 nm can be assigned to the emission of monomeric PDI

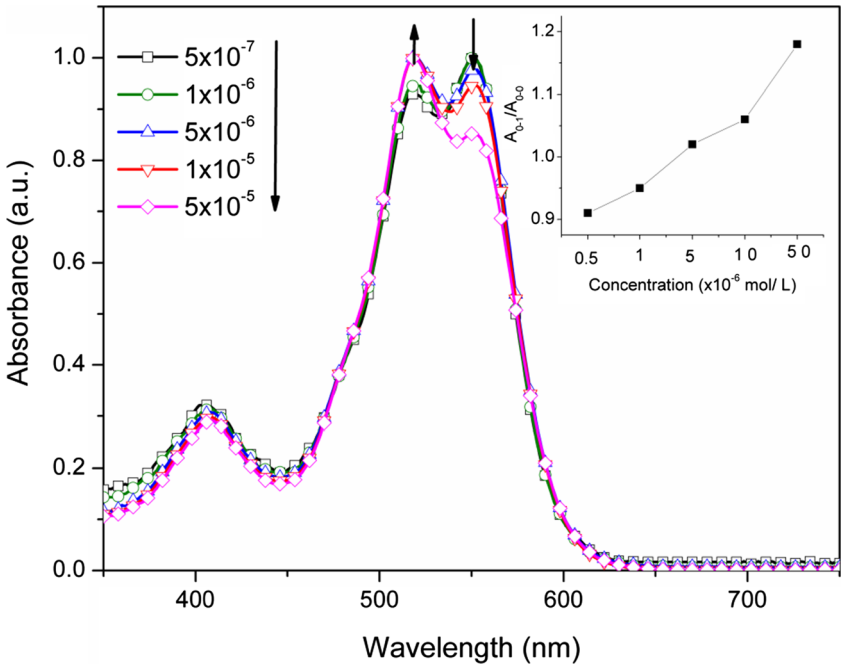

Fig. 5 The normalized concentration-dependent absorption spectra of trimer **1** in chloroform (from 5×10^{-7} to 5×10^{-5} mol L^{-1}) at room temperature

and is attributed to the non-aggregated trimer **1**. The band at 650 nm can be assigned to the emission of "excimer-like" states. Along with the concentration increase, all the trimer **1** molecules changed into aggregates and the emission from monomeric PDI at 560 nm disappear gradually, and only the emission from excimer-like states at 650 nm remains in the fluorescence spectrum.

The aggregation of trimer **1** in this THF/methanol mixed solvent is reversible as revealed by the temperature-dependent fluorescence spectra as shown in Fig. 9. At low temperatures, such as room temperature, the solution of trimer **1** in the mixed solvent gives a spectrum dominated by the emission from excimer-like states. However, the emission from monomeric PDI at 550–600 nm became the dominating component of the fluorescence when the temperature rises to 50 °C.

Both the absorption and fluorescence spectra of the diluted solution of trimer **2** in MCH (5×10^{-7} mol/L) (Fig. 10) are similar with those of trimer **1** in the mixed solvent of THF/methanol, which suggests the formation of H-type aggregates. The concentration decrease does not bring distinctive change

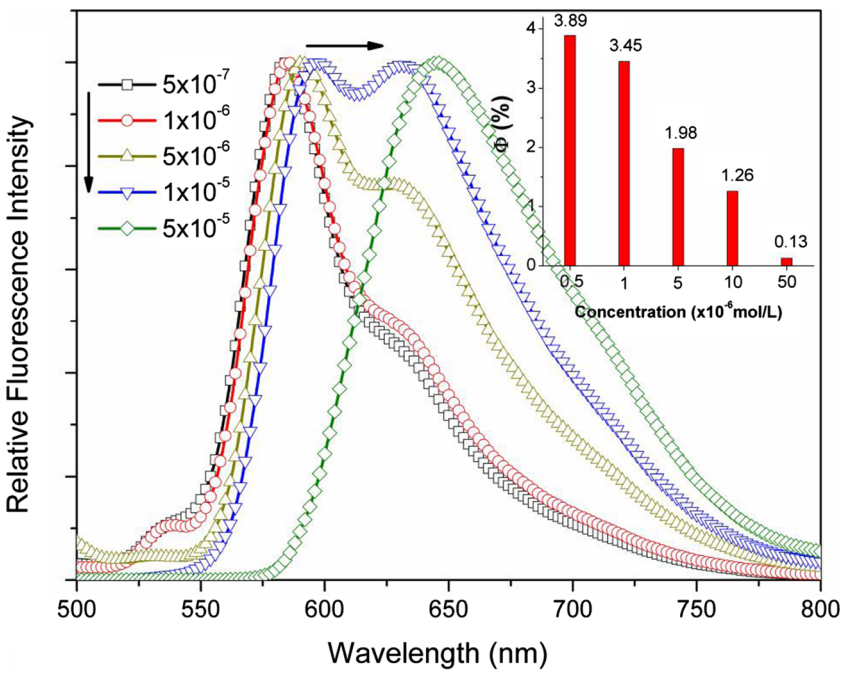

Fig. 6 The normalized concentration-dependent fluorescence spectra of timer **1** in chloroform (5×10^{-7}–5×10^{-7} mol/L) at room temperature

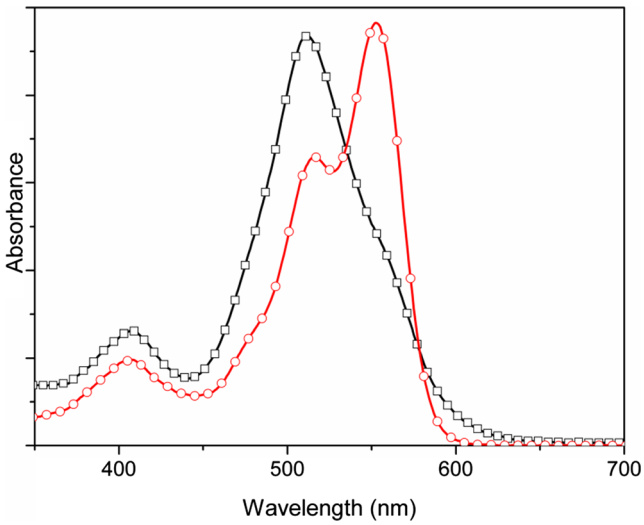

Fig. 7 Normalized absorption spectrum of trimer **1** (*black*, with *open squares*) in the mixed solvent of methanol and THF (methanol/THF 4:1; 1×10^{-6} mol/L). The absorption spectrum of monomer **3** (*red* with *open circles*) is also shown as comparison

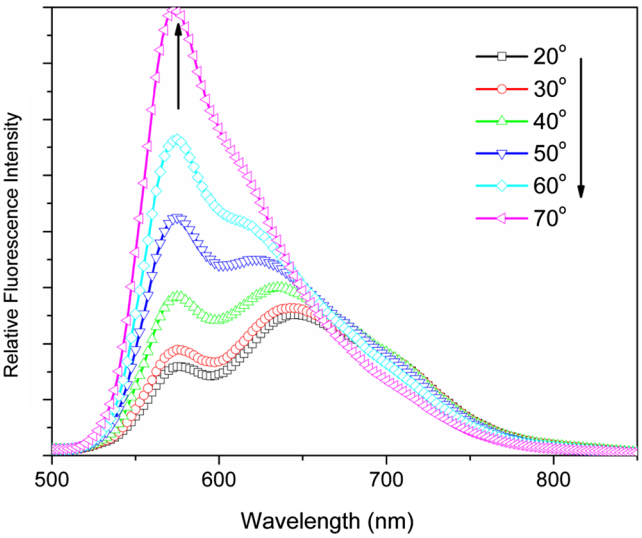

Fig. 9 The fluorescence spectra of trimer **1** in the mixture (5×10^{-6} mol L^{-1}) of methanol and THF (4:1) at different temperatures (λ_{ex}=410 nm)

on the absorption and the fluorescence spectra of trimer **2** in MCH (Fig. S5 in Supporting Information). This means that the aggregates formed by trimer **2** in the MCH solution are much stable than those by trimer **1** in the mixed solvent, and almost all the molecules of trimer **2** exists in the form of aggregates even in diluted solution. The fluorescence quantum yields of trimer **2** decrease remarkably along with concentration increase, which can be attributed to the enhanced interactions between the PDI subunits in the aggregates [36].

The temperature-dependent absorption spectra of trimer **2** in MCH reveal also no distinctive changes in shape as well as maximum emission wavelength along with temperature rising; only a slight increase of fluorescence quantum yield is observed (Fig. 11). It seems that the aggregates of trimer **2** are very stable and cannot be broken at elevated temperatures. This might be attributed to the long alkyl chains, which bring extra intermolecular interactions between the molecules of trimer **2**.

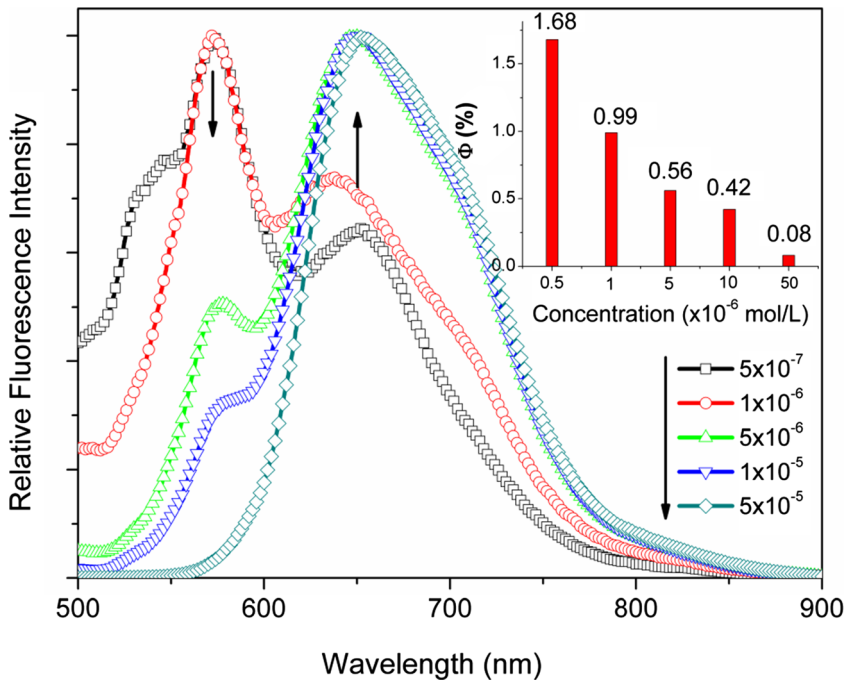

Fig. 8 The normalized concentration-dependent fluorescence spectra of trimer **1** in the mixed solvent of methanol and THF (4:1). The *inset* shows the fluorescence quantum yields (Φ) at different concentrations

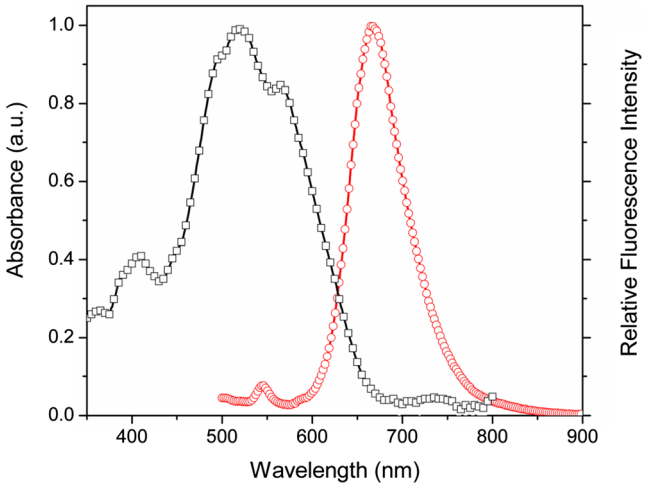

Fig. 10 Normalized absorption (*black* with *open squares*) and fluorescence (*red* with *open circles*) spectra of trimer **2** (5×10^{-7} mol/L) in diluted MCH solution

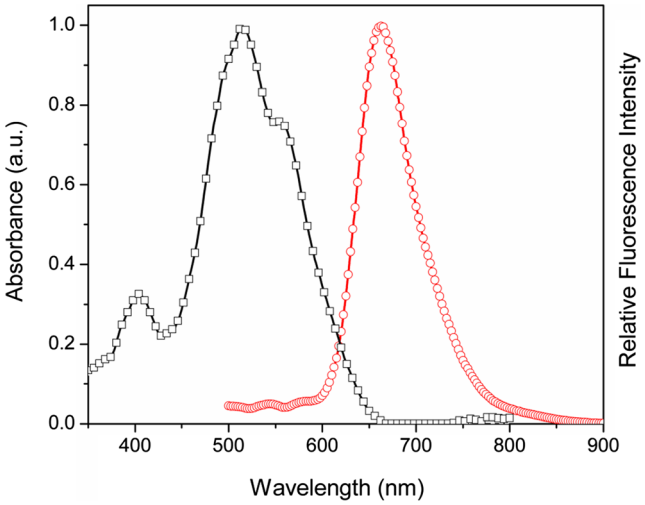

Fig. 12 Normalized absorption (*black*) and fluorescence (*red*) spectra of trimer **2** in toluene (5×10^{-6} mol L^{-1})

Besides, in MCH, trimer **2** can also form aggregates in toluene. The absorption and fluorescence spectra of trimer **2** in toluene resemble those of trimer **2** in MCH (Fig. 12). The temperature and concentration-dependent absorption and fluorescence spectra of trimer **2** in toluene did not show significant changes along with concentration and temperature change, suggesting the high stabilities for the aggregates of trimer **2** in toluene.

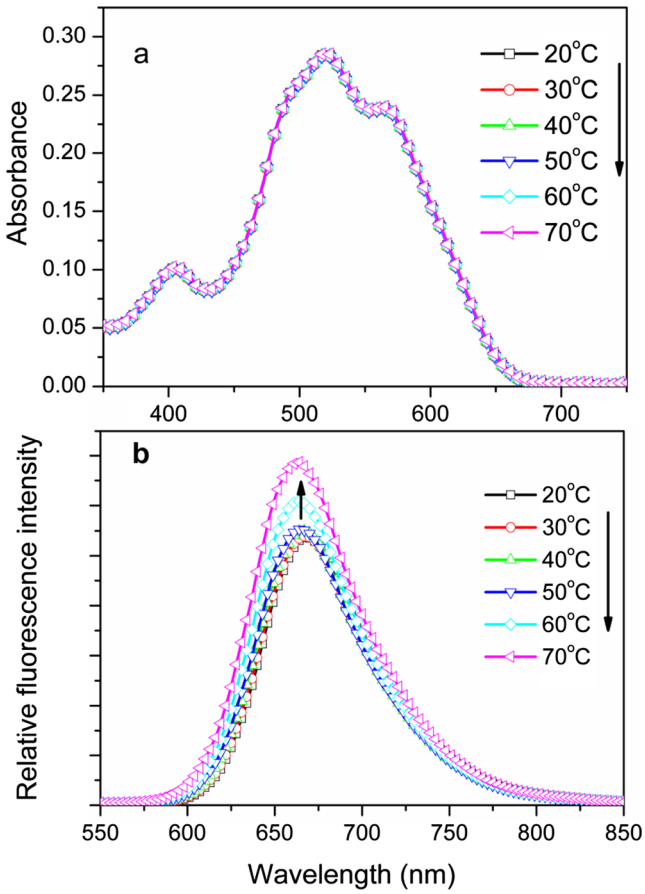

Fig. 11 Temperature-dependent absorption and fluorescence spectra of timer **2** in MCH (5×10^{-6} mol/L) at different temperatures

Gelating properties

Based on the good aggregation properties revealed by the spectroscopic results as presented above, we expect good gelating properties for both trimer **1** and trimer **2**. The gelating abilities are tested in several organic solvents. The samples are mixed with the solvent in a glass vial, and then, the mixture is heated until everything is dissolved. The mixture is then cooled to room temperature. After leaving the sample for 2 days at ambient temperature, we invert the vial to check the state of the solution. Trimer **1** can only form gel in the mixed solvent of methanol and THF (V_{MeOH}/V_{THF}=1:4). Trimer **2** can form gel in both MCH and toluene but does not in polar solvents, such as acetone, dioxane, and THF. The critical gelation concentrations [26] of trimer **1** in the mixed solvent are determined to be 2 mmol mL^{-1}, and trimer **2** in MCH is 3.37 mmol mL^{-1} at room temperature (Fig. 13). It is worth noting that the gelating process is thermally reversible. On heating, the gel can change into transparent solution and form gel again on cooling. The gels can also be broken by vigorously stirring and shaking.

The absorption and fluorescence spectra of the gels of trimer **1** and trimer **2** are shown in Fig. 14. The absorption spectrum of the gel of trimer **1** is similar with that of trimer **1** in the diluted mixed solvent (V_{MeOH}/V_{THF}=1:4), but with distinctive broadening on the absorption bands. The fluorescence spectrum of the gel of trimer **1** presents a further red-shifted emission peak (676 nm) compared with that in the diluted mixed solvent (652 nm), which can be attributed to the enhanced intermolecular aggregation of trimer **1** in the gel state. The absorption spectrum of the gel of trimer **2** is also identical

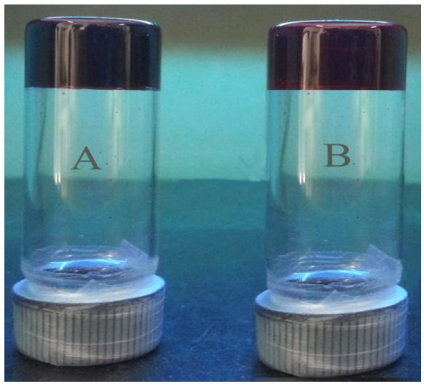

Fig. 13 Photographs of the gel of trimer **1** (**a**) in THF/methanol (4/1) and trimer **2** (**b**) in MCH

to that in MCH solution. The maximal emission peak of the gel of trimer **2** has red-shifted from 631 nm in MCH solution to 669 nm in the gel state, which can be ascribed similarly to the enhanced intermolecular aggregation of trimer **2** in gel [51].

The morphologies of the dried gels are examined by atomic force microscopy (AFM) (Fig. 15). Long fibers without obvious winding have been found in the image of the gel of timer **1**. But, in the image of the gel of trimer **2**, long fibers without definite end formed a network. These different morphologies

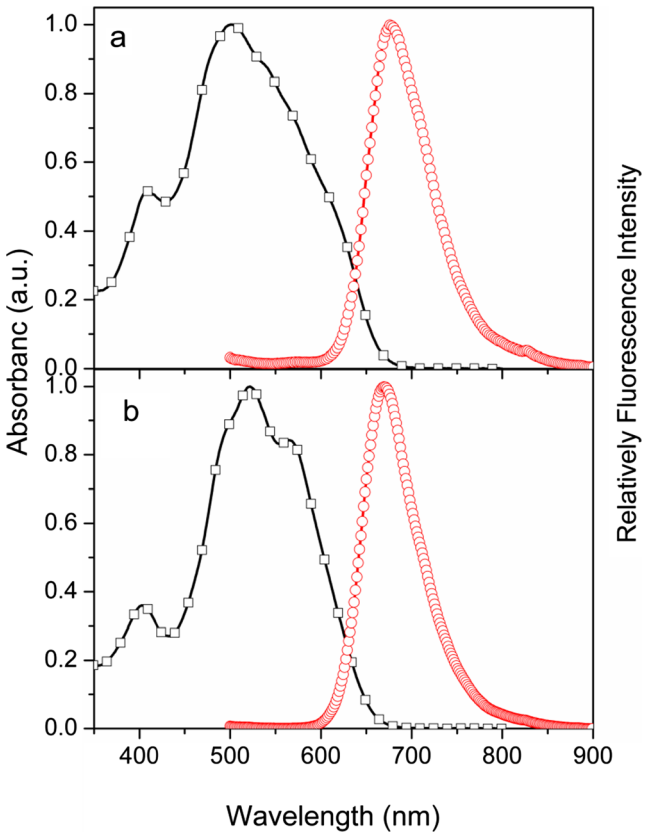

Fig. 14 Normalized absorption (*black*) and emission (*red*) spectra of the gels of trimer **1** (**a**, 2.0 mmol/mL) in THF/methanol (4:1) and trimer **2** (**b**, 3.37 mmol/mL) in MCH

can be assigned to the different molecular structure between trimers **1** and **2**. Two kinds of driving forces are working in the aggregation process of both trimer **1** and trimer **2**. They are π–π interactions between the PDI rings and hydrophobic interactions between the long alkyl chains. Because the π–π interactions between the PDI subunits are similar with each other, therefore, which will not bring large difference on the aggregation behavior between trimer **1** and trimer **2**. But, in trimer **1**, only one long alkyl chain connected to each of the three PDI subunits. The hydrophobic interactions between the long alkyl chains of different molecules are, therefore, small. But, in trimer **2**, there are three long alkyl chains that are connected to each PDI subunits, and the hydrophobic interactions between the molecules of trimer **2** are much stronger than those of trimer **1**. These strong hydrophobic interactions together with the π–π interactions drive the molecules of trimer **2** to form long fibers. Moreover, the efficient chain interdigitation between the fibers provides extra driving force for long fibers to weave into a network [35].

Hydrogen bonding may be another important driving force for the gelating of these two trimers in solvents because of the presence of the amide groups in these two compounds. Because trimer **1** can only form gel in the mixed solvent of methanol/THF, the hydrogen bonding should not be the important factor in the formation of gel because of the presence of proton solvent. However, timer **2** has extra three amide groups in its molecules, and therefore, its gelating process in non-polar and non-proton solvents is expected to be driven by the hydrogen bonds too. To verify this, the IR spectrum of the dried gel of trimer **2** was recorded, and the results are shown in Fig. S6 in Supporting Information. It can be seen that a distinctive band at about 3,500 cm^{-1} appears, which reveals the presence of hydrogen bonds in the gel and suggests that hydrogen bonding is indeed another driving force for the gelating of trimer **2** in non-polar solvents [18, 19].

XRD patterns

The internal structure of gels was further investigated by X-ray diffraction (XRD) experiments. Figure 16 shows the XRD patterns of the dried gel of trimer **1** and trimer **2**. In the XRD pattern of trimer **1**, a broad peak in the range of 2θ=15–25°, corresponding to a *d* space of about 0.42 nm, can be assigned to the liquid-like order of the alkyl chains [52]. In the low-angle region, two diffraction peaks are observed. The peak at 2θ=3.22° (*d*=2.74 nm) is roughly equal to the width of the molecules, and the peak at 6.43° (*d*=1.37 nm) is the second-order diffraction of the peak at 3.22°, which revealed that the molecules take an “edge-on” configuration on the surface of the substrate. Because the fibers are lying on the substrate with the long axis parallel to the surface of the substrate, therefore, it can conclude that the molecular plane of trimer **1** in the aggregates is perpendicular to the growing direction (long

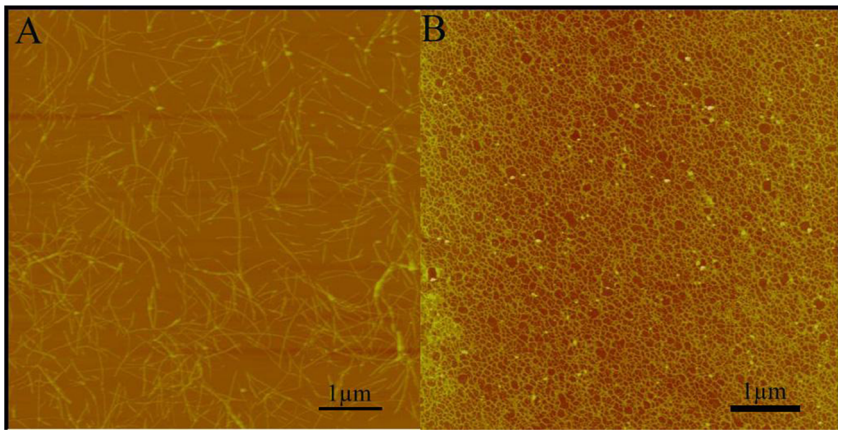

Fig. 15 AFM images of films formed from dropped diluted gel solutions of **a** trimer **1** in the mixture solvent of THF/methanol (4:1) and **b** trimer **2** in MCH onto the surface of a SiO_2 substrate and then volatilized slowly to dry

axis) of the fiber. A diffraction peak at about 2θ=28.51°, where the diffraction of π–π stacking of aromatic rings normally appears, is observed, which suggests the PDI units in the gel of trimer **1** packing with long-range order [53, 54]. This is in accordance with the morphology observation as mentioned above.

In the XRD pattern of trimer **2**, the broad peak with a *d* space of 0.315 nm can be assigned to the π–π stacking of aromatic rings [55]. In the low-angle region, a small diffraction peak at 2θ=2.41° (*d*=3.66 nm) may be ascribed to the diameter of the disk-like molecule of trimer **2**. But, the *d* value is smaller than the radius of the molecule calculated (Fig. 17b) based on an energy-minimized molecular structure (MM^+), which may be ascribed to alkyl chain interdigitation between the adjacent molecules.

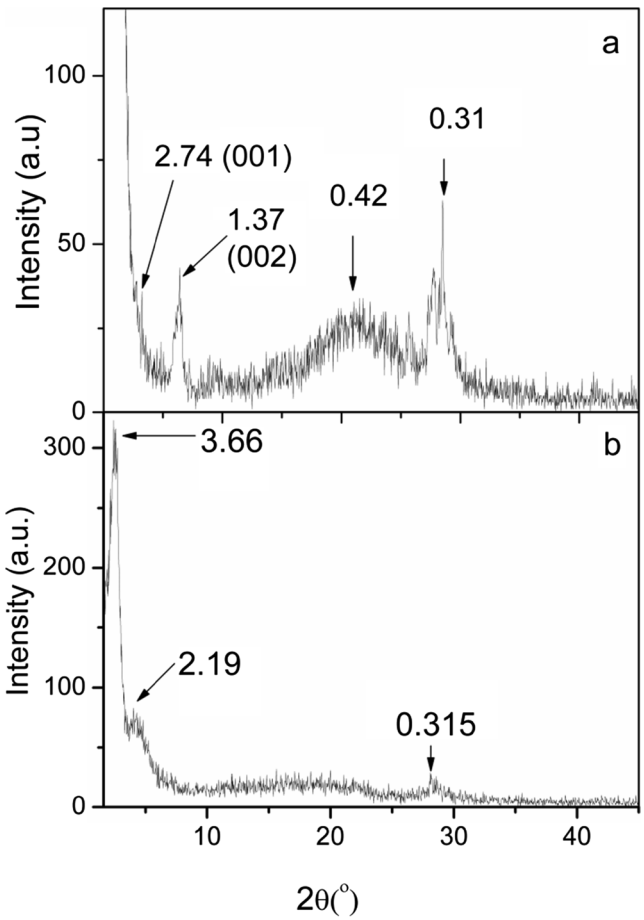

Fig. 16 XRD patterns for dried gels of trimer **1** (**a**) and trimer **2** (**b**)

Based on the results of the XRD, spectroscopic experiments, and morphology examination, we can draw a speculated microstructure for the molecular aggregates of trimer **1** and trimer **2** in gel, respectively. In the mixed solvent of THF and methanol, driven by the π–π interaction and hydrophobic interaction between the alkyl chains, the PDI subunits of trimer **1** stacked in a face-to-face way to form dimers. Along with concentration increase, the molecules of trimer **1** further self-assembled into linear fibers driven mainly by the π–π interaction between the PDI rings of different molecules. The thin linear fibers form large aggregates by interlacing. For the trimer **2**, the π–π interaction together with the strong hydrophobic interaction of the long alkyl chains drives the molecules to stack along the perpendicular direction of the molecular plane into slim fibers, and then, because of the interdigitation of the long alkyl chains of different fibers, the two-dimensional grid-like fibers formed finally.

Conclusions

Two new PDI trimers, trimer **1** and trimer **2**, containing different alkyl tails, are prepared. Due to the presence of efficient π–π interactions, the PDI subunits in these two compounds can form face-to-face stacked aggregates even in very dilute solutions. This result suggests that connection of multiple PDI subunits in one molecule can indeed enhance the interactions between the molecules and thus promote the aggregation of the molecules in solution. But, two trimers formed different fibers with different morphology due to the different number of alkyl side chains connected. Trimer **1** can form long fibers in concentrated solution driven mainly by the

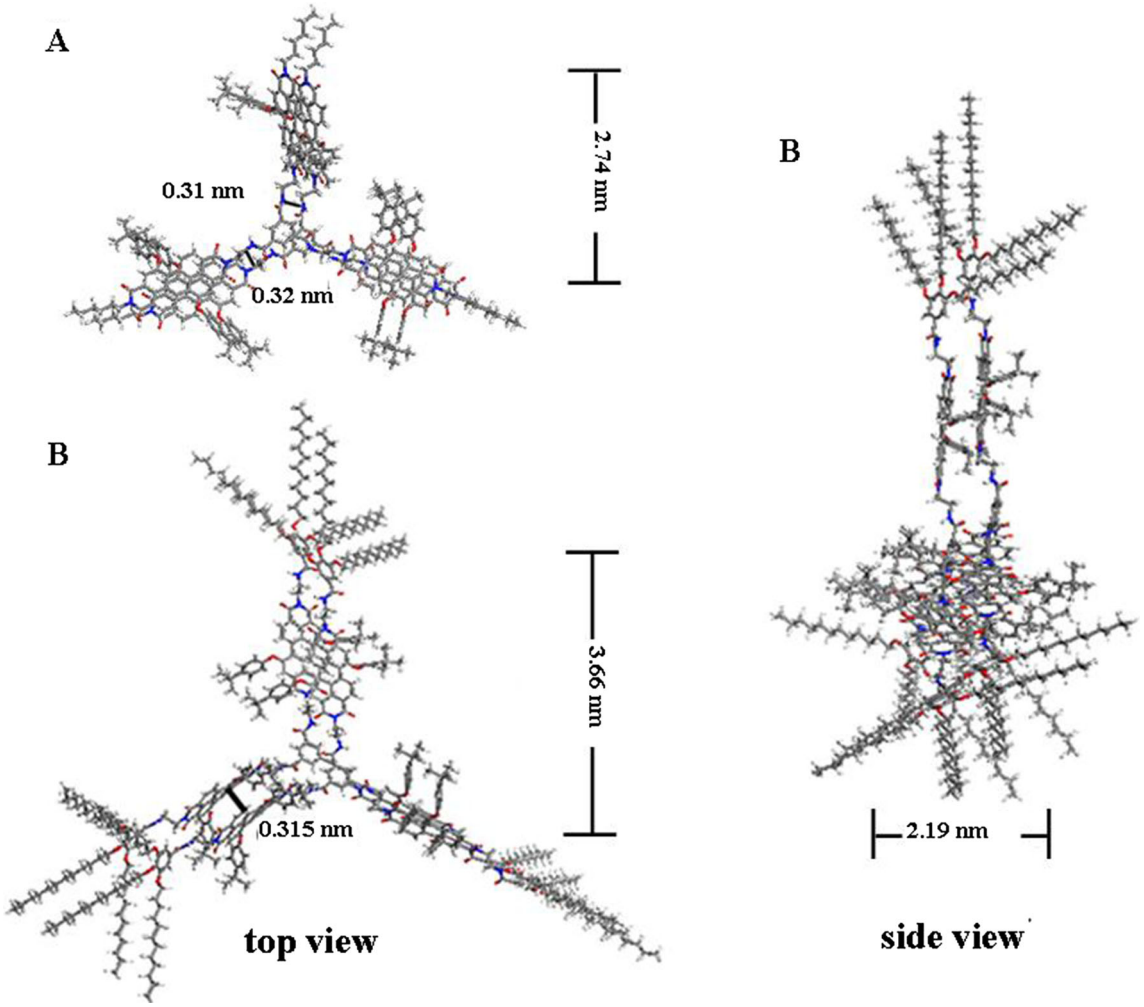

Fig. 17 The energy-minimized structure (MM^{+}) of the dimeric aggregates of trimer **1** (**a**) and trimer **2** (**b**)

π–π interactions. This makes it a good gelator for the mixed solvent of methanol and THF. Trimer **2**, which has three long alkyl chains connected at the end of the molecule, can form long fibers too, but because of the interdigitation of the long hydrophobic alkyl chains, the fibers tangle into a network.

Experimental

General methods

^{1}HNMR spectra were recorded at 300 MHz with the solvent peak as the internal standard (in $CDCl_3$). Electronic absorption spectra were recorded on a Hitachi 4100 spectrometer. The spectra of the extremely diluted solutions were recorded in a larger cuvette with a 5-cm light path. Fluorescence spectra were measured on an ISS K2 system. Fluorescence quantum yields were calculated with *N*,*N*,-dicyclohexyl-1,7-di(p-t-butyl-phenoxyl)-3,4,9,10-tetracarboxylic diimide (Φ_f=100 %) as the standard [56], and all samples were excited at 410 nm. MALDI-TOF mass spectra were obtained on a Bruker BIFLEX III mass spectrometer with acyano-4-hydroxycinnamic acid as matrix. The morphology of the dried gel on Si was studied in air by the use of a Veeco multimode atomic force microscope (AFM) in tapping mode. The low-angle X-ray diffraction (LAXD) experiment was carried out on a Rigaku $D/_{max\text{-}\gamma}B$ X-ray diffractometer.

Materials and methods

All solvents were of analytical grade and purified by using standard methods [57]. 1,7-Di(p-t-butyl-phenoxyl)-3,4,9,10-tetra-carboxylic dianhydried (**5**) [58], *N*-(2-aminoethyl)-3,4,5-tris(dodecyloxy)benzamide [31], *N*′-octyl-1,7-Di(p-t-butyl-phenoxyl)-3,4-dicarboxylic imide-9,10-dicarboxylic anhydride (**6**) [45], and *N*-(2-aminoethyl)-*N*′-hexyl-1,7-Di(p-t-butyl-phenoxyl)-3,4,9,10-

tetra-carboxylic diimide (**8**) [59] were synthesized by the procedures described previously.

Trimer 1 To a mixture of compound **8** (400 mg, 0.49 mmol) and 20 ml $CHCl_3$, trimesoyl chloride (43 mg, 0.16 mmol) in $CHCl_3$ (30 ml) was added drop by drop after the reaction flask was purged with N_2 for several times, and then, the reaction mixture was stirred continuously at room temperature overnight. After the solvent was evaporated, the residue was purified by column chromatography on silica gel ($CHCl_3$/methanol=99.2/0.8, *v*/*v* as eluent) to give trimer **1** (300 mg, 75 %) as red solid. ^{1}H NMR (300 MHz, $CDCl_3$): δ=9.4–9.0 (m, broad, 6H), 7.86–8.31 (s, broad, 6H), 7.79–7.86 (s, broad, 6H), 7.31–7.38 (m, 12H), 7.0–7.2(m, 12H) 6.81–6.83 (s, 3H), 4.35–4.47 (s, broad, 6H), 3.95 (s, 6H), 3.48–3.85 (broad, 6H), 1.8–1.2 (m, broad, 78H), and 0.86 (broad, 9H). MS (MALDI-TOF): *m*/*z*, calculated for $C_{165}H_{153}N_9O_{21}$: 2,596.1, found 2,597.2 [M+H]$^+$; elemental analysis (%) calculated for $C_{165}H_{153}N_9O_{21}$: C 76.28, H 5.94, N 4.85; found: C 76.14, H 5.87, N 4.88.

Compound 7 To a mixture of 1,7-di(p-t-butyl-phenoxyl)-3,4,9,10-tetracarboxylic dianhydried (344 mg, 0.5 mmol) in 30 ml dried pyridine, a solution of *N*-(2-aminoethyl)-3,4,5-tris(dodecyloxy)benzamide (165 mg, 0.23 mmol) in 10 ml dried pyridine was added drop by drop. The mixture was refluxed at 115 °C for 1.5 h. After cooling to room temperature, the solvent was evaporated. The residue was purified by column chromatography on silica gel (CH_2Cl_2 as eluent) to give compound **7** (32.5 mg, 10 %). ^{1}H NMR (300 MHz, $CDCl_3$): δ=9.65 (m, 2H), 8.59 (m, 2H), 8.35 (d, 2H), 7.50–7.53 (d, 4H), 7.13 (d, 4H), 6.89 (s, 2H), 6.75 (t, 1H), 4.45 (t, 2H), 3.91 (t, 6H), 3.78 (br, 2H), 1.8–1.2 (m, 78H), and 0.87 (m, 9H). MS (MALDI-TOF): *m*/*z*, calculated for $C_{89}H_{114}N_2O_{11}$: 1,387.91, found 1,387.67 [M$^+$]; elemental analysis (%) calculated for $C_{89}H_{114}N_2O_{11}$: C 77.02, H 8.28, N 2.02; found: C 77.05, H 8.46, N 2.12.

Compound 9 To a mixture of ethylenediamine (1 ml) and 30 ml $CHCl_3$, compound **7** (140 mg, 0.1 mmol) in 10 ml $CHCl_3$ was added drop by drop with continues stirring at room temperature. The resulted mixture was stirred continually at room temperature under a nitrogen atmosphere overnight. After the solvent was evaporated, the residue was purified by column chromatography on silica gel (methanol/chloroform=3:95) to give compound **9** (108 mg, 75 %). ^{1}H NMR (300 MHz, $CDCl_3$): δ=9.60–9.64 (m, 2H), 8.55–8.63 (m, 2H), 8.34 (d, 2H), 7.44–7.48 (d, 4H), 7.12 (d, 4H), 6.89 (s, 2H), 4.49–5.1 (m, 3H), 4.45 (t, 2H), 4.17–4.20 (t, 2H), 3.91 (t, 6H), 3.11(t, 2H), 2.45 (t, 2H), 1.8–1.2 (m, 78H), and 0.87 (m, 9H). MS (MALDI-TOF): *m*/*z*, calculated for $C_{89}H_{114}N_2O_{11}$: 1429, found 1428.6; [M$^+$]; elemental analysis (%) calculated for $C_{91}H_{120}N_4O_{10}$: C 76.44, H 8.46, N 3.92; found: C 76.65, H 8.23, N 3.79.

Trimer 2 To a mixture of compound **9** (240 mg, 0.17 mmol), triethylamine (1 ml) and 20 ml $CHCl_3$, trimesoyl chloride (14 mg 0.057 mmol) was added drop by drop with continuous stirring at room temperature. The resulting mixture was stirred continually at room temperature under a nitrogen atmosphere overnight. After the solvent was evaporated, the residue was purified by column chromatography on silica gel ($CHCl_3$/MeOH=08. 99.2, *v*/*v* as eluent) to give trimer **2** (134 mg, 60 %). ^{1}H NMR spectrum of trimer **2** in $CDCl_3$ (c=3×10^{-4} M) shows very broad peaks, suggesting the formation of molecular aggregates [34]. ^{1}H NMR (300 MHz, $CDCl_3$): δ=9.15–9.28 (s, broad, 6H), 8.0–8.15 (s, broad, 6H), 7.98 (s, broad, 6H), 7.39–7.47 (m, 12H), 7.00–7.04 (m, 12H), 6.99 (s, 6H), 6.95 (s, 3H), 4.45 (s, broad, 6H), 3.95 (t, 18H), 3.48–3.85 (s, broad, 12H), 1.8–1.2 (m, broad, 234H), and 0.89 (broad, 27H). MS (MALDI-TOF): *m*/*z*, calculated for $C_{282}H_{360}N_{12}O_{33}$: 4445.6, found 4448.3 [M$^+$]; elemental analysis (%) calculated for $C_{282}H_{360}N_{12}O_{33}$: C 76.18, H 8.16, N 3.79; found: C 76.14, H 8.32, N 3.52.

Acknowledgments Financial support from the Natural Science Foundation of China (with Grand No. 91233108 and 21173136), the National Basic Research Program of China (973 Program: 2012CB93280), and the Graduate Independent Innovation Foundation of Shandong University are gratefully acknowledged.

References

1. Stangl J, Holý V, Bauer G (2004) Structural properties of self-organized semiconductor nanostructures. Rev Mod Phys 76:725–783
2. Lu H, Hofmann T, Yager KG, Black CT, Ocko BM (2011) Nanoimprint-induced molecular orientation in semiconducting polymer nanostructures. ACS Nano 5:7532–7538
3. Dholakia GR, Fan W, Koehne J, Han J, Meyyappan M (2004) Transport in self-assembled molecular wires: effect of packing and order. Phys Rev B 69:1534021
4. Wong LN, Hu CH, Paradise R, Zhu ZN, Shtukenberg A, Kahr B (2012) Relationship between tribology and optics in thin films of mechanically oriented nanocrystals. J Am Chem Soc 134:12245–12251
5. Kamat PV (2007) Meeting the clean energy demand: nanostructure architectures for solar energy conversion. J Phys Chem C 111:2834–2860
6. Peet J, Heeger AJ, Bazan GC (2009) "Plastic" solar cells: self-assembly of bulk heterojunction nanomaterials by spontaneous phase separation. Acc Chem Res 42:1700–1708
7. Gledhill SE, Scott B, Gregg BA (2005) Organic and nano-structured composite photovoltaics: an overview [Quick Edit] [CiTO]. J Mater Res 20:3167–3179
8. Dalacu D, Reimer ME, Frederick S, Kim D, Lapointe J, Poole PJ, Aers GC, Williams RL, McKinnon WR, Korkusinski M, Hawrylak P (2010) Directed self-assembly of single quantum dots for telecommunication wavelength optical devices. Laser Photonics Rev 4:283–289
9. Romeo HE, Hoppe CE, Lopez-Quintela MA, Williams RJJ, Minaberry Y, Jobbagy M (2012) Directional freezing of liquid crystalline systems: from silver nanowire/PVA aqueous dispersions to

highly ordered and electrically conductive macroporous scaffolds. J Mater Chem 22:9195–9201
10. Prehm M, Götz G, Bäuerle P, Liu F, Zeng X, Ungar G, Tschierske C (2007) Complex liquid-crystalline superstructure of a π-conjugated oligothiophene. Angew Chem Int Ed 46:7856–7859
11. Liu Y, Flood AH, Bonvallet PA, Vignon SA, Northrop BH, Tseng HR, Jeppesen JO, Huang TJ, Brough B, Baller M, Magonov S, Solares SD, Goddard WA, Ho CM, Stoddart JF (2005) Linear artificial molecular muscles. J Am Chem Soc 127:9745–9759
12. Sui R, Charpentier P (2012) Synthesis of metal oxide nanostructures by direct sol–gel chemistry in supercritical fluids. Chem Rev 112: 3057–3082
13. Richert L, Vetrone F, Yi JH, Zalzal SF, Wuest JD, Rosei F, Nanci A (2008) Surface nanopatterning to control cell growth. Adv Mater 20: 1488–1492
14. Gröschel AH, Schacher FH, Schmalz H, Borisov OV, Zhulina EB, Walther A, Müller AHE (2012) Precise hierarchical self-assembly of multicompartment micelles. Nat Commun 3:710
15. Xu H, Hong R, Lu TX, Uzun O, Rotello VM (2006) Recognition-directed orthogonal self-assembly of polymers and nanoparticles on patterned surfaces. J Am Chem Soc 128:3162–3163
16. Ajayaghosh A, George SJ, Praveen VK (2003) Gelation-assisted light harvesting by selective energy transfer from an oligo(p-phenylenevinylene)-based self-assembly to an organic dye. Angew Chem Int Ed 42:332–335
17. Sugiyasu KS, Fujita N, Shinkai S (2004) Visible-light-harvesting organogel composed of cholesterol-based perylene derivatives. Angew Chem Int Ed 43:1229–1232
18. Rao MR, Sun S-S (2013) Supramolecular assemblies of amide-derived organogels featuring rigid π-conjugated phenylethynyl frameworks. Langmuir 29:15146–15158
19. Shirakawa M, Kawano S-I, Fujita N, Sada K, Shinkai S (2003) Hydrogen-bond-assisted control of H versus J aggregation mode of porphyrins stacks in an organogel system. J Org Chem 68:5037–5044
20. Tamaru S-I, Uchino S-Y, Takeuchi M, IkedaM M, Hatano T, Shinkai S (2002) A porphyrin-based gelator assembly which is reinforced by peripheral urea groups and chirally twisted by chiral urea additives. Tetrahedron Lett 43:3751–3755
21. Dammer C, Maldivi P, Terech P, Guenet J-M (1995) Rheological study of a bicopper tetracarboxylate/decalin jelly. Langmuir 11: 1500–1506
22. Sagawa T, Fukugawa S, Yamada T, Ihara H (2002) Self-assembled fibrillar networks through highly oriented aggregates of porphyrin and pyrene substituted by dialkyl l-glutamine in organic media. Langmuir 18:7223–7228
23. Tamaru S-I, Nakamura M, Takeuchi M, Shinkai S (2001) Rational design of a sugar-appended porphyrin gelator that is forced to assemble into a one-dimensional aggregate. Org Lett 3:3631–3634
24. Van Nostrum CF, Picken S, Schouten A-J, Nolte RJM (1995) Synthesis and supramolecular chemistry of novel liquid crystalline crown ether-substituted phthalocyanines: toward molecular wires and molecular ionoelectronics. J Am Chem Soc 117:9957–9965
25. Engelkamp H, Middelbeek S, Nolte RJM (1999) Self-assemble of disk-shaped molecules to coiled-coil aggregates with tunsble helicity. Science 284:785–788
26. Ajayaghosh A, George SJ (2001) First phenylenevinylene based organogels: self-assembled nanostructures via cooperative hydrogen bonding and π-stacking. J Am Chem Soc 123:5148–5149
27. Schoonbee FS, Van Esch JH, Wegewijs B, Rep DBA, De Haas MP, Klapwijk TM, Kellogg RM, Feringa BL (1999) Effizienter intermolekularer Ladungstransport in selbstorgaisierten Fasern aus Mono-und Bithiophenen mit zwei Harnstoffeinheiten. Angew Chem 111:1486–1490
28. Yagai S, Usui M, Seki T, Murayama H, Kikkawa Y, Uemura S, Karatsu T, Kitamura A, Asano A, Seki S (2012) Supramolecularly engineered perylene bisimide assemblies exhibiting thermal transition from columnar to multilamellar structures. J Am Chem Soc 134: 7983–7994
29. Krieg E, Shirman E, Weissman H, Shimoni E, Wolf SG, Pinkas I, Rybtchinski B (2009) Supramolecular gel based on a perylene diimide dye: multiple stimuli responsiveness, robustness, and photofunction. J Am Chem Soc 131:14365–14373
30. Würthner F, Hanke B, Lysetska M, Lambright G, Harms GS (2005) Gelation of a highly fluorescent urea-functionalized perylene bisimide dye. Org Lett 7:967–970
31. Li X-Q, Zhang X, Ghosh S, Würthner F (2008) Highly fluorescent lyotropic mesophases and organogels based on J-aggregates of core-twisted perylene bisimide dyes. Chem Eur J 14:8074–8078
32. Wu H, Xue L, Shi Y, Chen Y, Li X (2011) Organogels based on J- and H-type aggregates of amphiphilic perylenetetracarboxylic diimides. Langmuir 27:3074–3308
33. Xue L, Wang Y, Chen Y, Li X (2010) Aggregation of wedge-shaped perylenetetracarboxylic diimides with a different number of hydrophobic long alkyl chains. J Coll Interface Sci 350:523–529
34. Van Hameren R, Schön P, Buul AM, Hoogboom J, Lazarenko Sergiy V, Gerritsen JW, Engelkamp H, Christianen PCM, Heus HA, Maan JC, Rasing T, Speller S, Rowan AE, Elemans JAAW, Nolte RJM (2006) Macroscopic hierarchical surface patterning of porphyrin trimers via self-assembly and dewetting. Science 314:1433–1436
35. Che Y, Datar A, Balakrishnan K, Zang L (2007) Thermally activated electron transport in single redox molecules. J Am Chem Soc 129: 7234–7235
36. Wang Y, Chen Y, Li R, Wang S, Su W, Ma P, Wasielewski M, Li X, Jiang J (2007) Amphiphilic perylenetretracarboxyl diimide dimer and its application in field effect transistor. Langmuir 23:5836–5842
37. Feng J, Liang B, Wang D, Wu H, Xue L, Li X (2008) Synthesis and aggregation behavior of perylenetetracarboxylic diimide trimers with different substituents at bay positions. Langmuir 24:11209–11215
38. Li X-Q, Stepanenko V, Chen Z, Prins P, Siebbeles LDA, Würthner F (2006) Functional organogels from highly efficient organogelator based on perylene bisimide semiconductor. Chem Commun 1(37): 3871–3873
39. Kazmaier PM, Hoffmann R (1994) A theoretical study of crystallochromy. Quantum interference effects in the spectra of perylene pigments. J Am Chem Soc 116:9684–9691
40. Giaimo JM, Lockard JV, Sinks LE, Scott AM, Wilson TM, Wasielewski M (2008) Excited singlet states of covalently bound, cofacial dimers and trimers of perylene-3,4:9,10-bis(dicarboximide)s. J Phys Chem A 112:2322–2330
41. Wang W, Li L-S, Helms G, Zhou H-H, Li DQ (2003) To fold or to assemble? J Am Chem Soc 125:1120–1121
42. Balakrishnan K, Datar A, Oitker R, Chen H, Zuo J, Zang L (2005) Nanobelt self-assembly from an organic n-type semiconductor: propoxyethyl-PTCDI. J Am Chem Soc 127:10496–10497
43. Balakrishnan K, Datar A, Naddo T, Huang J, Oitker R, Yen M, Zhao J, Zang L (2006) Effect of side-chain substituents on self-assembly of perylene diimide molecules: morphology control. J Am Chem Soc 128:7390–7398
44. Chen Y, Chen L, Qi G, Wu H, Zhang Y, Xue L, Zhu P, Ma P, Li X (2010) Self-assembled organic-inorganic hybrid nanocomposite of a perylenetetracarboxylic diimide derivative and CdS. Langmuir 26: 12473–12478
45. Xue L, Wu H, Shi Y, Liu H, Chen Y, Li X (2011) Supramolecular organogels based on perylenetetracarboxylic diimide dimer or hexamer. Soft Matter 7:6213–6221
46. Sinks LE, Rybtchinski B, Iimura M, Jones BA, Goshe AJ, Zuo XB, Tiede DM, Li XY, Wasielewski MR (2005) Self-assembly of photofunctional cylindrical nanostructures based on perylene-3,4:9,10-bis(dicarboximide). Chem Mater 17: 6295–6303

47. Wang Y, Chen H, Wu H, Li X, Weng Y (2009) Fluorescence quenching in a perylenetetracarboxylic diimide trimer. J Am Chem Soc 131:30–31
48. Feng J, Zhang Y, Zhao C, Li R, Xu W, Li X, Jiang J (2008) Cyclophanes of perylene tetracarboxylic diimide with different substituents at bay positions. Chem Eur J 14:7000–7010
49. Li X, Sinks LE, Rybtchinski B, Wasielewski M (2004) Ultrafast aggregate-to-aggregate energy transfer within self-assembled light-harvesting columns of zinc phthalocyanine tetrakis(perylenediimide). J Am Chem Soc 126:10810–10811
50. Ghosh S, Li X, Stepanenko V, Würthner F (2008) Control of H- and J-type pi stacking by peripheral alkyl chains and self-sorting phenomena in perylene bisimide homo- and heteroaggregates. Chem Eur J 14:11343–11357
51. Liu H, Shen L, Cao Z, Li X (2014) Covalently linked perylenetertracarboxylic diimide dimers and trimers with rigid "J-tape". Phys Chem Chem Phys. doi:10.1039/C4CP01002G
52. Chen Z, Stepanenko V, Dehm V, Prins P, Siebbeles LDA, Seibt J, Marquetand P, Engel V, Würthner F (2007) Photoluminescence and conductivity of self-assembled pi-pi stacks of perylene bisimide dyes. Chem Eur J 13:436–449
53. Klebe G, Graser F, Hadicke E, Berndt (1989) Crystallochromy as a solid-state effect: correlation of molecular conformation, crystal packing and colour in perylene-3,4: 9,10-bis (dicarboximide) pigments. J Acta Cryst B45:69–77
54. Graser F, Hädicke E (1980) Kristallstruktur und farbe bei perylen-3, 4: 9, 10-bis (dicarboximid)-pigmenten. Liebigs Ann Chem 23:1994–2011
55. Yelamaggad CV, Achalkumar AS, Rao DSS, Prasad SK (2007) Monodispersive linear supermolecules stabilizing unusual fluid layered phases. J Org Chem 72:8308–8318
56. Zhao CC, Zhang YX, Li RJ, Li XY, Jiang JZ (2007) Di(alkoxy)- and di(alkylthio)-substituted perylene-3,4;9,10-tetracarboxy diimides with tunable electrochemical and photophysical properties. J Org Chem 72:2402–2410
57. Perrin DD, Armarego WLF, Perrin DR (1980) Purification of laboratory chemicals. Pergamon, Oxford
58. Lukas AS, Zhao Y, Miller SE, Wasielewski M (2002) Biomimetic electron transfer using low energy excited states: a green perylene-based analogue of chlorophyll a. J Phys Chem B 106:1299–1306
59. Zhou J, Xue L, Shi Y, Li X, Xue Q, Wang S (2012) Synthesis and self-assembly of perylenetetracarboxylic diimide derivatives with helical oligo(l-lactic acid)$_n$ segments. Langmuir 28:14386–14394